

# Phase transitions in strongly coupled three-dimensional $Z(N)$ lattice gauge theories at finite temperature

O. Borisenko<sup>1†</sup>, V. Chelnokov<sup>1\*</sup>, G. Cortese<sup>2††</sup>, R. Fiore<sup>3¶</sup>, M. Gravina<sup>4‡</sup>, A. Papa<sup>3¶</sup>, I. Surzhikov<sup>1\*\*</sup>

<sup>1</sup> *Bogolyubov Institute for Theoretical Physics,  
National Academy of Sciences of Ukraine,  
03680 Kiev, Ukraine*

<sup>2</sup> *Instituto de Física Teórica UAM/CSIC,  
Cantoblanco, E-28049 Madrid, Spain  
and Departamento de Física Teórica,  
Universidad de Zaragoza, E-50009 Zaragoza, Spain*

<sup>3</sup> *Dipartimento di Fisica, Università della Calabria,  
and Istituto Nazionale di Fisica Nucleare, Gruppo collegato di Cosenza  
I-87036 Arcavacata di Rende, Cosenza, Italy*

<sup>4</sup> *Department of Physics, University of Cyprus, P.O. Box 20357, Nicosia, Cyprus*

## Abstract

We perform an analytical and numerical study of the phase transitions in three-dimensional  $Z(N)$  lattice gauge theories at finite temperature for  $N > 4$  exploiting equivalence of these models with a generalized version of the two-dimensional vector Potts models in the limit of vanishing spatial coupling. In this limit the Polyakov loops play the role of  $Z(N)$  spins. The effective couplings of these two-dimensional spin models are calculated explicitly. It is argued that the effective spin models have two phase transitions of BKT type. This is confirmed by large-scale Monte Carlo simulations. Using a cluster algorithm we locate the position of the critical points and study the critical behavior across both phase transitions in details. In particular, we determine various critical indices, compute the helicity modulus, the average action and the specific heat. A scaling formula for the critical points with  $N$  is proposed.

---

*e-mail addresses:*

<sup>†</sup>oleg@bitp.kiev.ua, <sup>\*</sup>vchelnokov@i.ua, <sup>††</sup>cortese@unizar.es, <sup>¶</sup>fiore, papa @cs.infn.it,  
<sup>‡</sup>gravina@ucy.ac.cy, <sup>\*\*</sup>i\_van\_go@inbox.ru

# 1 Introduction

The phase structure of three-dimensional ( $3d$ ) pure  $Z(N)$  lattice gauge theories (LGTs) has been the subject of an intensive study for more than three decades. It is well known by now that the zero-temperature models possess a single phase transition which disappears in the limit  $N \rightarrow \infty$  [1]. Thus, the  $U(1)$  LGT has a single confined phase in agreement with theoretical results [2]. The deconfinement phase transition at finite temperature is well understood and studied for  $N = 2, 3$ . These models belong to the universality class of  $2d$   $Z(N)$  spin models and exhibit a second order phase transition in agreement with the Svetitsky-Yaffe conjecture [3]. Much less is known about the finite-temperature deconfinement transition when  $N > 4$ . The Svetitsky-Yaffe conjecture is known to connect critical properties of  $3d$   $Z(N)$  LGTs with the corresponding properties of  $2d$  spin models, if they share the same global symmetry of the action. It is widely expected, and in many cases proved by either analytical or numerical methods, that some  $2d$   $Z(N > 4)$  spin models (like the vector Potts model) have two phase transitions of infinite order, known as the Berezinskii-Kosterlitz-Thouless (BKT) phase transitions. Then, according to the conjecture, the phase transitions in some  $3d$   $Z(N > 4)$  gauge models at finite temperature could exhibit two phase transitions as well. Moreover, if the correlation length diverges when approaching the critical point, these transitions should be of the BKT type and belong to the universality class of the corresponding  $2d$   $Z(N)$  spin models.

The BKT phase transition is known to take place in a variety of  $2d$  systems: certain spin models,  $2d$  Coulomb gas, sine-Gordon model, Solid-on-Solid model, etc. The most elaborated case is the  $2d$   $XY$  model [4, 5, 6]. There are several indications that this type of phase transition is not a rare phenomenon in gauge models at finite temperature - one can argue that in some  $3d$  lattice gauge models the deconfinement phase transition is of BKT type as well. A well known example is the deconfinement phase transition in the  $U(1)$  LGT. Indeed, certain analytical [3, 7, 8] as well as numerical results [9, 10] unambiguously indicate the BKT nature of the phase transition<sup>1</sup>.

Many details of the critical behavior of  $2d$   $Z(N)$  spin models are well known - see the review in Ref. [11]. The  $Z(N)$  spin model in the Villain formulation has been studied analytically in Refs. [12, 13, 14, 15, 16, 17]. It was shown that the model has at least two phase transitions when  $N \geq 5$ . The intermediate phase is a massless phase with power-like decay of the correlation function. The critical index  $\eta$  has been estimated both from the renormalization group (RG) approach of the Kosterlitz-Thouless type and from the weak coupling series for the susceptibility. It turns out that  $\eta(\beta_c^{(1)}) = 1/4$  at the transition point from the strong coupling (high-temperature) phase to the massless

---

<sup>1</sup>It should be noted, however, that the numerical results of [10] point to a critical index  $\eta$  larger than its  $XY$  value by almost a factor of 2 for  $N_t = 8$ . Therefore, the question of the universality remains open for this model.

phase, *i.e.* the behavior is similar to that of the  $XY$  model. At the transition point  $\beta_c^{(2)}$  from the massless phase to the ordered low-temperature phase one has  $\eta(\beta_c^{(2)}) = 4/N^2$ . A rigorous proof that the BKT phase transition does take place, and so that the massless phase exists, has been constructed in Ref. [18] for both Villain and standard formulations of the vector Potts model. Universality properties of vector Potts models were studied via Monte Carlo simulations in Ref. [19] for  $N = 6, 8, 12$  and in Refs. [20, 21, 22, 23] for  $N = 5, 7, 17$ . Results for the critical indices  $\eta$  and  $\nu$  agree well with the analytical predictions obtained from the Villain formulation of the model.

We expect that  $3d$   $Z(N)$  gauge models at finite temperature exhibit the same critical properties as  $Z(N)$  spin models in two dimensions. In particular, gauge models with  $N > 4$  may possess two phase transitions of the BKT type. On the basis of the Svetitsky-Yaffe conjecture the critical behavior of the gauge model in this case is governed by the  $2d$   $Z(N)$  spin model. In particular, one expects the following values of critical indices:  $\nu = 1/2$ ,  $\eta = 1/4$  at the first transition and  $\nu = 1/2$ ,  $\eta = 4/N^2$  at the second transition. To the best of our knowledge this scenario was not verified in the literature by either analytical or numerical means. The main goal of the present paper is to fill this gap and to study the nature of deconfining phase transitions in  $3d$   $Z(N)$  LGTs.

The fact that the BKT transition has infinite order makes it hard to study its properties using analytical methods. In most of the cases studied one uses a renormalization group (RG) technique like in Ref. [12]. Unfortunately, there are no direct ways to generalize transformations of Ref. [12], leading to RG equations, to  $3d$   $Z(N)$  LGTs except for the limiting case  $N \rightarrow \infty$ . To study the phase structure of these models we need numerical simulations. Here, however, another problem appears related to the very slow, logarithmic convergence to the thermodynamic limit in the vicinity of the BKT transition. It is thus necessary to use both large-scale simulations and combine them with the finite-size scaling methods. For a full finite-temperature gauge model this is an ambitious program, especially if one wants to study several values of  $N$ . We have therefore decided to utilize an approach developed by some of the present authors in Refs. [9, 10] and to divide the whole investigation into two steps. The finite-temperature model is formulated on anisotropic lattice with different spatial and temporal couplings. Here, following [9], as a first step, we study the limit of vanishing spatial coupling. Since this approximation does not affect the global symmetry properties of the model, we hope that in this limit the model belongs to the same universality class as the full theory. It is well known that for both three- and four-dimensional gauge models at finite temperature this is indeed the case, at least for  $N = 2, 3, 4$ . Furthermore, in this limit the gauge model can be mapped onto a generalized  $Z(N)$  spin model in  $2d$ . Thus, this investigation sheds some light on the details of the critical behavior of the general Potts model, *i.e.* beyond the vector Potts model, which is usually considered in the literature. In the present paper we study the phase transitions in models with  $N = 5, 7$  in great details and in addition we locate

critical points of the models with  $N = 9, 13$ . Our computations are performed on lattices with temporal extent  $N_t = 2, 4$  and with spatial size in the range  $L \in [128 - 2048]$ .

This paper is organized as follows. In Section 2 we formulate our model and study some of its properties analytically. In particular, we establish the exact relation with a generalized  $2d$   $Z(N)$  spin model and discuss some of the RG predictions regarding the critical behavior. Also, we give simple analytical estimates for the critical couplings. In Section 3 we present the setup of Monte Carlo simulations, define the observables used in this work and present the numerical results of simulations for  $N = 5, 7$ . In Section 4 we present results for the critical points in the models with  $N = 9, 13$  and discuss the scaling of the critical points with  $N$ . Our conclusions and perspectives are given in Section 5.

## 2 Analytical considerations

### 2.1 Relation of the $3d$ $Z(N)$ LGT to a generalized $2d$ $Z(N)$ vector model

We work on a  $3d$  lattice  $\Lambda = L^2 \times N_t$  with spatial extension  $L$  and temporal extension  $N_t$ ;  $\vec{x} = (x_0, x_1, x_2)$ , where  $x_0 \in [0, N_t - 1]$  and  $x_1, x_2 \in [0, L - 1]$  denote the sites of the lattice and  $e_n$ ,  $n = 0, 1, 2$ , denotes a unit vector in the  $n$ -th direction. Periodic boundary conditions (BC) on gauge fields are imposed in all directions. The notations  $p_t$  ( $p_s$ ) stand for the temporal (spatial) plaquettes,  $l_t$  ( $l_s$ ) for the temporal (spatial) links.

We introduce conventional plaquette angles  $s(p)$  as

$$s(p) = s_n(x) + s_m(x + e_n) - s_n(x + e_m) - s_m(x) . \quad (1)$$

The  $3d$   $Z(N)$  gauge theory on an anisotropic lattice can generally be defined as

$$Z(\Lambda; \beta_t, \beta_s; N) = \prod_{l \in \Lambda} \left( \frac{1}{N} \sum_{s(l)=0}^{N-1} \right) \prod_{p_s} Q(s(p_s)) \prod_{p_t} Q(s(p_t)) . \quad (2)$$

The most general  $Z(N)$ -invariant Boltzmann weight with  $N - 1$  different couplings is

$$Q(s) = \exp \left[ \sum_{k=1}^{N-1} \beta_p(k) \cos \frac{2\pi k}{N} s \right] . \quad (3)$$

The Wilson action corresponds to the choice  $\beta_p(1) = \beta_p$ ,  $\beta_p(k) = 0$ ,  $k = 2, \dots, N - 1$ . The  $U(1)$  gauge model is defined as the limit  $N \rightarrow \infty$  of the above expressions.

To study the phase structure of  $3d$   $Z(N)$  LGTs in the strong coupling limit ( $\beta_s = 0$ ) one can map the gauge model to a generalized  $2d$  spin  $Z(N)$  model with the action

$$S = \sum_x \sum_{n=1}^2 \sum_{k=1}^{N-1} \beta_k \cos \left( \frac{2\pi k}{N} (s(x) - s(x + e_n)) \right) . \quad (4)$$

The effective coupling constants  $\beta_k$  are derived from the coupling constant  $\beta_t \equiv \beta$  of the  $Z(N)$  LGT, using the following equation (the Wilson action is used for the gauge model):

$$\beta_k = \frac{1}{N} \sum_{p=0}^{N-1} \ln(Q_p) \cos \left( \frac{2\pi pk}{N} \right) , \quad (5)$$

where

$$Q_k = \sum_{p=0}^{N-1} \left( \frac{B_p}{B_0} \right)^{N_t} \cos \left( \frac{2\pi pk}{N} \right) , \quad (6)$$

$$B_k = \sum_{p=0}^{N-1} \exp \left[ \beta \cos \left( \frac{2\pi p}{N} \right) \right] \cos \left( \frac{2\pi pk}{N} \right) . \quad (7)$$

These equations can be easily obtained in a few steps following similar computations for  $3D$   $SU(N)$  model in the same limit  $\beta_s = 0$  (see, for example, Ref. [24] and references therein):

- Fourier expansion of the original Boltzmann weight;
- Integration over spatial gauge fields; this leads to an effective  $2d$  model for the Polyakov loops with the Boltzmann weight  $Q(s(x) - s(x + e_n))$  defined in (6);
- Exponentiation and re-expansion in a new Fourier series.

## 2.2 Renormalization group and critical behavior

To gain some information on the critical behavior of the gauge model at  $\beta_s = 0$ , one can perform the RG study of the theory. Let us consider the  $2d$  model obtained after integration over spatial gauge fields,

$$Z(\Lambda; \beta; N) = \prod_{x \in \Lambda} \left( \frac{1}{N} \sum_{s(x)=0}^{N-1} \right) \prod_l \left[ \sum_{k=0}^{N-1} (B_k)^{N_t} \cos \left( \frac{2\pi k}{N} (s(x) - s(x + e_n)) \right) \right] . \quad (8)$$

The coefficients  $B_k \equiv B_k(\beta)$  are given in (7) and can be represented as

$$B_k = \sum_{r=-\infty}^{\infty} I_{Nr+k}(\beta) . \quad (9)$$

Here,  $I_k(x)$  is the modified Bessel function. The spin variables  $s(x)$  can be associated with the Polyakov loops of the original model.

The RG equations can be obtained only for the Villain formulation of the model. Replacing the Bessel function with its asymptotics and using the Poisson summation formula, one finds

$$\begin{aligned} Z(\Lambda; \beta; N) &= \prod_{x \in \Lambda} \left( \frac{1}{N} \sum_{s(x)=0}^{N-1} \right) \\ &\times \prod_l \left[ \sum_{m=-\infty}^{\infty} \exp \left[ -\frac{1}{2} \beta_{\text{eff}} \left( \frac{2\pi}{N} (s(x) - s(x + e_n)) + 2\pi m \right)^2 \right] \right] . \end{aligned} \quad (10)$$

This is nothing but the Villain formulation of  $2d$   $Z(N)$  vector model with  $\beta_{\text{eff}}$  defined as

$$\beta_{\text{eff}} = \beta/N_t . \quad (11)$$

The RG equations for the model (11) have been constructed in [12]. Their analysis has been performed by us in a recent work [23]. Therefore, all the conclusions as to the critical behavior remain valid in the present case. We shortly list the main results below:

1. The critical RG trajectories in the planes  $(\beta_{\text{eff}}, y)$  and  $(\beta_{\text{eff}}, z)$ , where  $y, z$  are the activities of the vortex configurations, coincide with those of the  $2d$   $Z(N)$  vector spin model;
2. The critical index  $\nu$  has been computed numerically from the RG equations for a variety of  $N$ . It takes on the value  $1/2$  for all  $N$  considered, in particular for  $N = 5, 7$ ;
3. The calculation of the two-point correlation function reveals that the index  $\eta$  is equal to  $1/4$  at the first transition point, while  $\eta = 4/N^2$  at the second critical point [12]. The same behavior is valid for the correlation of the Polyakov loops in our model;
4. In [23] we have calculated the dependence of the critical points on  $N$ . These scaling formulae are expected to hold in the present case for any fixed  $N_t$  and will be the subject of the discussion in Section 4.

### 2.3 Estimation of the critical points

The location of the critical points in  $3d$   $Z(N)$  LGTs for  $N > 4$  is unknown. Therefore, before presenting numerical results, it is instructive to give some simple analytical predictions for the critical values of  $\beta^{\text{crit}}$  for different values  $N_t$ . Such a prediction could serve then as the starting point for the numerical search of the critical points. Following [9], such critical values can be easily estimated if one knows  $\beta^{\text{crit}}$  for  $N_t = 1$ . Since the model with  $N_t = 1$  coincides with the  $2d$   $Z(N)$  model, approximate critical points for other values of  $N_t$  can be computed from the equality

$$\frac{B_1}{B_0}(\beta^{\text{crit}}) = \left[ \frac{B_1}{B_0}(x) \right]^{N_t}, \quad (12)$$

where  $x$  on the right-hand side denotes the unknown critical point. Solving the last equation numerically one finds  $x$ . As for the critical points  $\beta^{\text{crit}}$  at  $N_t = 1$ , we use our previous estimates from [21]. As it will be seen below, the predicted values are in a reasonable agreement with the numerical results. Table 1 summarizes approximate analytical predictions for the critical couplings at the two transitions, denoted by  $\beta_c^{(1)}$  and  $\beta_c^{(2)}$ , respectively; the last two columns show Monte Carlo values.

Table 1: Values of  $\beta_c^{(1)}$  and  $\beta_c^{(2)}$  expected for  $N_t = 1, 2, 4$  in  $Z(N)$  with  $N = 5, 7$ .

$N$	$N_t$	$\beta_c^{(1)}$	$\beta_c^{(2)}$	$\beta_c^{(1)}_{\text{MC}}$	$\beta_c^{(2)}_{\text{MC}}$
5	1	-	-	1.051(1)	1.105(1)
5	2	1.8393	1.9057	1.87(1)	1.940(7)
5	4	2.7761	2.8515	2.813(3)	2.898(4)
7	1	-	-	1.111(1)	1.88(8)
7	2	1.9861	3.1303	2.031(7)	3.366(7)
7	4	3.2995	4.9669	3.406(8)	5.158(7)

## 3 Numerical results

### 3.1 Setup of the Monte Carlo simulation

To study the phase transitions we used the cluster algorithm described in [21]. The model is studied on a square  $L \times L$  lattice  $\Lambda$  with periodic BC. Simulations were carried on for  $N_t = 2, 4$ , but could easily be done also for other values of  $N_t$ , since the parameter

$N_t$  appears only in the definition of the couplings (5). As original action of the gauge model we used the conventional Wilson action. For each Monte Carlo run the typical number of generated configurations was  $10^6$ , the first  $5 \times 10^4$  of them being discarded to ensure thermalization. Measurements were taken after 10 updatings and the uncertainty on primary observables was estimated by the jackknife method combined with binning.

We considered the following observables:

- complex magnetization  $M_L = |M_L|e^{i\psi}$ ,

$$M_L = \sum_{x \in \Lambda} \exp\left(\frac{2\pi i}{N} s(x)\right); \quad (13)$$

- population  $S_L$ ,

$$S_L = \frac{N}{N-1} \left( \frac{\max_{i=0, N-1} n_i}{L^2} - \frac{1}{N} \right), \quad (14)$$

where  $n_i$  is number of  $s(x)$  equal to  $i$ ;

- real part of the rotated magnetization  $M_R = |M_L| \cos(N\psi)$  and normalized rotated magnetization  $m_\psi = \cos(N\psi)$ ;
- susceptibilities of  $M_L$ ,  $S_L$  and  $M_R$ :  $\chi_L^{(M)}$ ,  $\chi_L^{(S)}$ ,  $\chi_L^{(M_R)}$ ,

$$\chi_L^{(\cdot)} = L^2 (\langle \cdot^2 \rangle - \langle \cdot \rangle^2); \quad (15)$$

- Binder cumulants  $U_L^{(M)}$  and  $B_4^{(M_R)}$ ,

$$\begin{aligned} U_L^{(M)} &= 1 - \frac{\langle |M_L|^4 \rangle}{3 \langle |M_L|^2 \rangle^2}, \\ B_4^{(M_R)} &= \frac{\langle |M_R - \langle M_R \rangle|^4 \rangle}{\langle |M_R - \langle M_R \rangle|^2 \rangle^2}; \end{aligned} \quad (16)$$

- helicity modulus  $\Upsilon$ ,

$$\Upsilon = \langle e \rangle - L^2 \beta \langle s^2 \rangle, \quad (17)$$

where

$$e \equiv \frac{1}{L^2} \sum_{\langle ij \rangle_x} \cos(\theta_i - \theta_j), \quad s \equiv \frac{1}{L^2} \sum_{\langle ij \rangle_x} \sin(\theta_i - \theta_j), \quad \theta_i \equiv \frac{2\pi}{N} s(i)$$

and the notation  $\langle ij \rangle_x$  means nearest-neighbors spins in the  $x$ -direction.



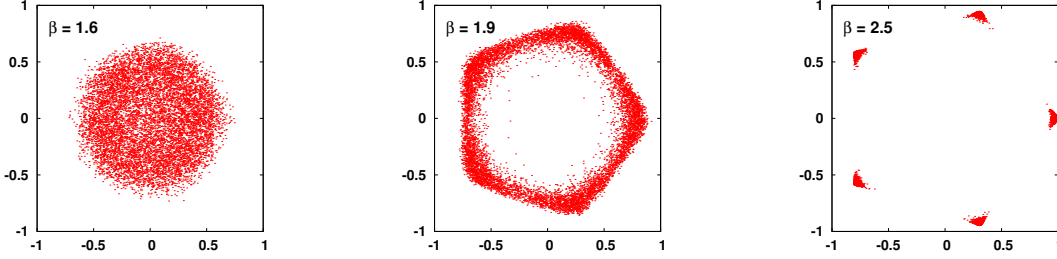


Figure 1: Scatter plot of the complex magnetization  $M_L$  at  $\beta=1.6$ ,  $1.9$  and  $2.5$  in  $Z(5)$  on a  $16^2 \times 2$  lattice.

### 3.2 Determination of the critical couplings

A clear indication of the three-phase structure emerges from the inspection of the scatter plot of the complex magnetization  $M_L$  at different values of  $\beta$ : as we move from low to high  $\beta$ , we observe the transition from a disordered phase (uniform distribution around zero) through an intermediate phase (ring distribution) up to the ordered phase ( $N$  isolated spots), as Fig. 1 shows for the case of  $Z(5)$  on a  $16^2 \times 2$  lattice.

The first and most important numerical task is to determine the value of the two critical couplings in the thermodynamic limit,  $\beta_c^{(1)}$  and  $\beta_c^{(2)}$ , that separate the three phases. To this aim we have adopted several methods, which we list here:

- Methods for the determination of  $\beta_c^{(1)}$ :
  - (a) locate the position  $\beta_{pc}^{(1)}(L)$  of the peak of the susceptibility  $\chi_L^{(M)}$  of the complex magnetization  $|M_L|$  on lattices with various spatial size and find  $\beta_c^{(1)}$  by a fit with the following scaling function, dictated by the essential scaling:

$$\beta_{pc}^{(1)} = \beta_c^{(1)} + \frac{A}{(\ln L + B)^{\frac{1}{\nu}}} \quad , \quad (18)$$

taking  $\nu$  equal to  $1/2$ ;

- (b) estimate the crossing point of the curves giving the behavior of the Binder cumulant  $U_L^{(M)}$  versus  $\beta$  on lattices with different spatial size  $L$  or, alternatively, search for the value of  $\beta_c^{(1)}$  which optimizes the overlap of these curves when they are plotted against  $(\beta - \beta_c^{(1)})(\ln L)^{1/\nu}$ , with  $\nu$  fixed at  $1/2$ ;

- (c) consider the helicity modulus  $\Upsilon$  near the phase transition and define  $\beta_{pc}^{(1)}(L)$  as the value of  $\beta$  such that  $\eta(\beta) \equiv 1/(2\pi\beta\Upsilon) = 1/4$  on the lattice with spatial size  $L$  [25], then find  $\beta_c^{(1)}$  by a fit with the scaling function

$$\beta_{pc}^{(1)} = \beta_c^{(1)} + \frac{A}{\ln L + B} \quad , \quad (19)$$

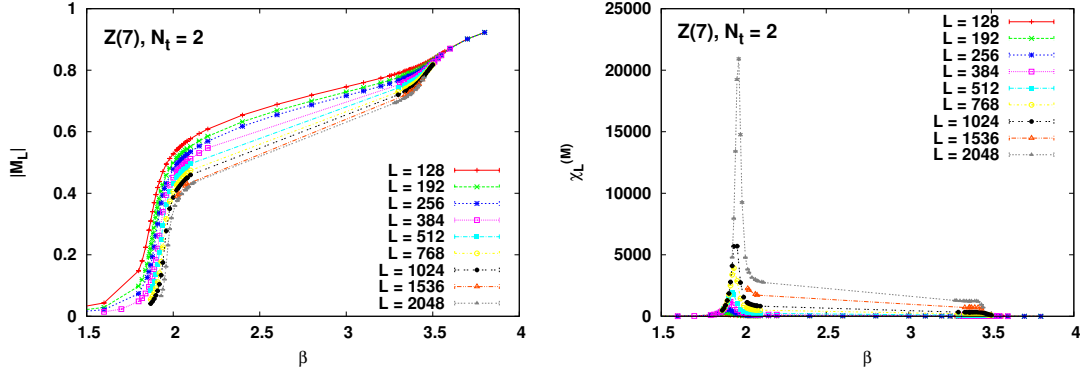


Figure 2: Behavior of  $M_L$  and of its susceptibility versus  $\beta$  in  $Z(7)$  on lattices with  $N_t = 2$  and  $L$  ranging from 128 to 2048.

valid under the assumption that the phase transition belongs to the  $XY$  universality class.

- Methods for the determination of  $\beta_c^{(2)}$ :
  - (d) same as the method (a) using instead the susceptibility  $\chi_L^{(S)}$  of the population  $S_L$ ;
  - (e) same as the method (b) using instead simultaneously the Binder cumulant  $B_4^{(M_R)}$  and the order parameter  $m_\psi$ .

As an illustration of the methods (a) and (d), we show in Figs. 2 and 3 the behavior of  $M_L$  (and of its susceptibility) and that of  $S_L$  (and of its susceptibility) versus  $\beta$  in  $Z(7)$  on lattices with  $N_t = 2$  and  $L$  ranging from 128 to 2048. In Table 2 we summarize all the values of  $\beta_{pc}^{(1)}(L)$  and  $\beta_{pc}^{(2)}(L)$  found in this work for the application of methods (a) and (d) in  $Z(N)$  with  $N = 5, 7$  for  $N_t = 2, 4$ .

As an illustration of the method (b), we show in Fig. 4 the behavior of  $U_L^{(M)}$  versus  $\beta$  in  $Z(7)$  on lattices with  $N_t = 2$  and  $L$  ranging from 128 to 2048. Similarly, as an illustration of the method (e), we show in Figs. 5 and 6 the behavior of  $B_4^{(M_R)}$  and of  $m_\psi$  versus  $\beta$  in  $Z(5)$  on lattices with  $N_t = 4$  and  $L$  ranging from 128 to 2048.

As an illustration of the method (c), we show in Fig. 7 the behavior of the helicity modulus  $\Upsilon$  versus  $\beta$  along with the line  $\Upsilon = 1/(2\pi\beta\eta)$ ,  $\eta = 1/4$ , describing pseudocritical points, in  $Z(5)$  and in  $Z(7)$  on lattices with  $N_t = 2, 4$  and several values of the spatial extension  $L$ . For larger values of  $L$  only the points around the intersection were simulated.

Finally, we report in Table 3 the determinations of the critical couplings  $\beta_c^{(1)}$  and  $\beta_c^{(2)}$  in  $Z(N)$  with  $N=5$  and  $7$  for  $N_t=2$  and  $4$ , specifying the adopted method.

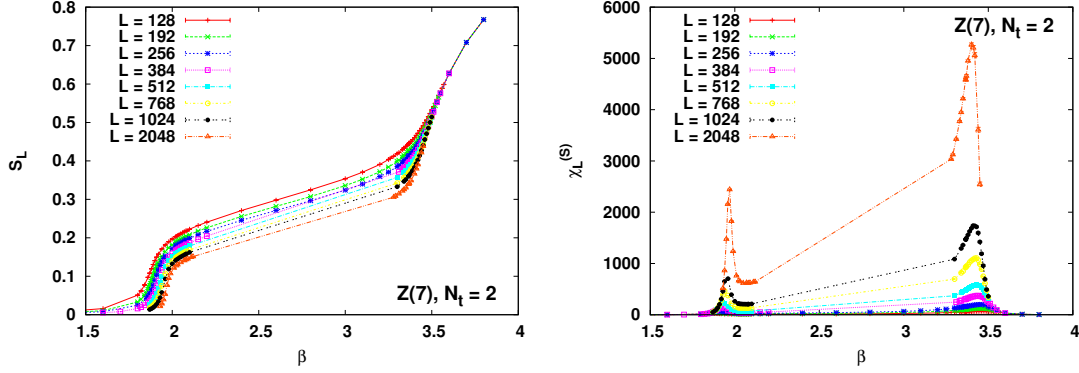


Figure 3: Behavior of  $S_L$  and of its susceptibility versus  $\beta$  in  $Z(7)$  on lattices with  $N_t = 2$  and  $L$  ranging from 128 to 2048.

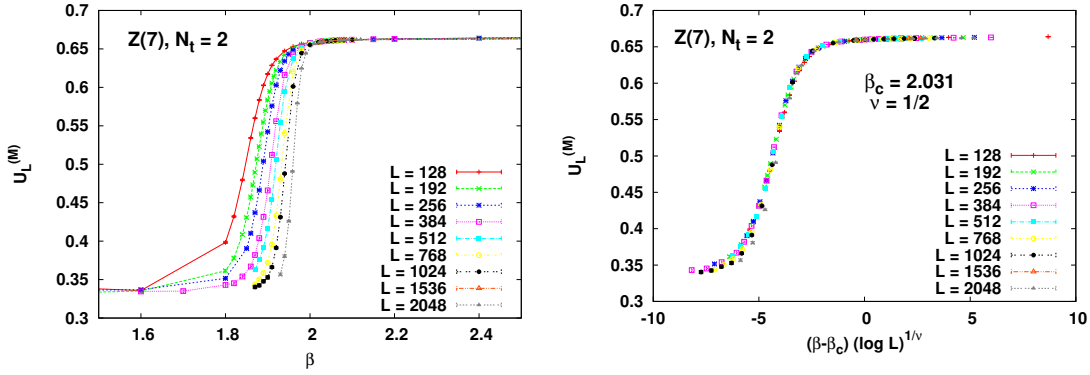


Figure 4: Binder cumulant  $U_L^{(M)}$  as function of  $\beta$  (left) and of  $(\beta - \beta_c)(\ln L)^{1/\nu}$  (right) in  $Z(7)$  on lattices with  $N_t = 2$  and  $L$  ranging from 128 to 2048.

Table 2: Summary of all the determinations of  $\beta_{\text{pc}}^{(1)}$  and  $\beta_{\text{pc}}^{(2)}$  in  $Z(N)$  on lattices with size  $L^2 \times N_t$ .

$N$	$N_t$	$L$	$\beta_{\text{pc}}^{(1)}$	$\beta_{\text{pc}}^{(2)}$
5	2	128	1.7656(1)	1.9773(5)
		192	1.7808(1)	1.9740(3)
		256	1.7910(1)	1.9713(4)
		384	1.80124(7)	1.9689(5)
		512	1.80774(6)	1.9658(3)
		768	1.81540(5)	1.9626(2)
		1024	1.82013(4)	1.9614(4)
		2048	1.83001(5)	
5	4	16	2.4913(9)	
		32	2.5928(6)	
		64	2.6538(5)	
		128	2.692(1)	2.9376(8)
		192	2.7131(8)	2.934(2)
		256	2.7226(7)	2.928(1)
		384	2.7357(7)	2.927(2)
		512		2.921(2)
		768		2.920(3)
1024		2.917(2)		
7	2	128	1.8644(4)	3.461(2)
		192	1.8873(2)	3.454(1)
		256	1.9011(2)	3.443(2)
		384	1.9184(2)	3.433(1)
		512	1.9289(2)	3.427(2)
		768	1.9421(2)	3.420(2)
		1024	1.9504(5)	3.416(2)
7	4	128	3.14(1)	5.257(1)
		192	3.18(1)	5.242(2)
		256	3.20(1)	5.2371(7)
		384	3.2220(2)	5.223(2)
		512	3.2392(1)	5.216(2)
		768	3.26024(6)	5.209(2)
		1024	3.2737(3)	5.198(2)

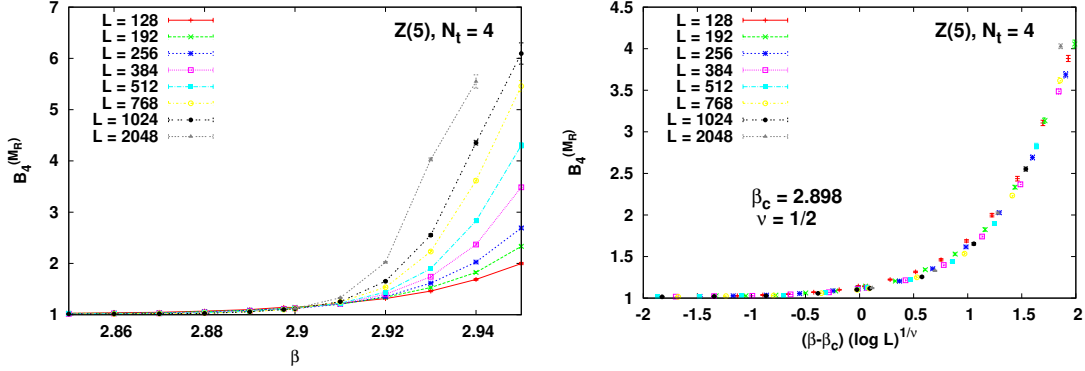


Figure 5: Binder cumulant  $B_4^{(M_R)}$  as a function of  $\beta$  (left) and of  $(\beta - \beta_c)(\ln L)^{1/\nu}$  (right) in  $Z(5)$  on lattices with  $N_t = 4$  and  $L$  ranging from 128 to 2048.

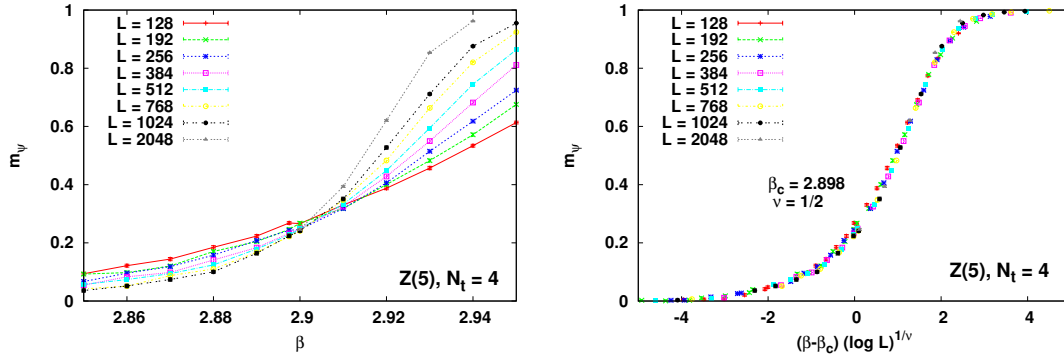


Figure 6:  $m_\psi$  as a function of  $\beta$  (left) and of  $(\beta - \beta_c)(\ln L)^{1/\nu}$  (right) in  $Z(5)$  on lattices with  $N_t = 4$  and  $L$  ranging from 128 to 2048.

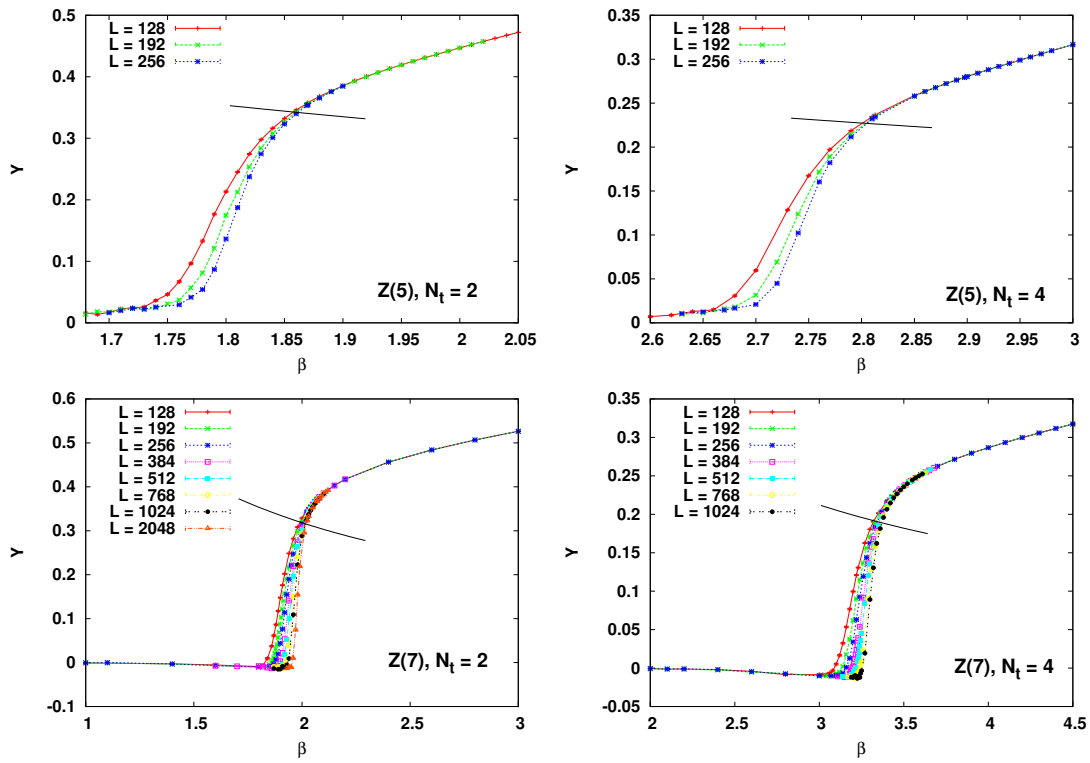


Figure 7: Helicity modulus as a function of  $\beta$  in  $Z(5)$  with  $N_t = 2$  (top left), in  $Z(5)$  with  $N_t = 4$  (top right), in  $Z(7)$  with  $N_t = 2$  (bottom left) and in  $Z(7)$  with  $N_t = 4$  (bottom right).

Table 3: Summary of the determinations of  $\beta_c^{(1)}$  and  $\beta_c^{(2)}$  in  $Z(N)$  on lattices with size  $L^2 \times N_t$ . The fourth (sixth) column gives the method adopted to find  $\beta_c^{(1)}$  ( $\beta_c^{(2)}$ ).

$N$	$N_t$	$\beta_c^{(1)}$	method	$\beta_c^{(2)}$	method
5	2	1.878(2)	a	1.91(6)	d
		1.87(1)	b	1.940(7)	e
		1.8801(7)	c		
5	4	2.832(3)	a	2.88(3)	d
		2.813(3)	b	2.898(4)	e
		2.829(1)	c		
7	2	2.070(2)	a	3.31(9)	d
		2.031(7)	b	3.366(7)	e
		2.069(1)	c		
7	4	3.47(1)	a	5.0(2)	d
		3.406(8)	b	5.158(7)	e
		3.4782(8)	c		

### 3.3 Determination of critical indices at the two transitions

Once critical couplings have been estimated, we are able to extract some critical indices and check the hyperscaling relation.

We start the discussion from the first transition. According to the standard finite-size scaling (FSS) theory, the equilibrium magnetization  $|M_L|$  at criticality should obey the relation  $|M_L| \sim L^{-\beta/\nu}$ , if the spatial extension  $L$  of the lattice is large enough<sup>2</sup>. Therefore, we fit data of  $|M_L|$  at  $\beta_c^{(1)}$  on all lattices with size  $L$  not smaller than a given  $L_{\min}$  with the scaling law

$$|M_L| = AL^{-\beta/\nu} \ln^r L, \quad (20)$$

where a non-zero value for  $r$  takes into account the possibility of logarithmic corrections [26, 27].

The FSS behavior of the susceptibility  $\chi_L^{(M)}$  is given by  $\chi_L^{(M)} \sim L^{\gamma/\nu}$ , where  $\gamma/\nu = 2 - \eta$  and  $\eta$  is the magnetic critical index. Therefore we fit data of  $\chi_L^{(M)}$  at  $\beta_c^{(1)}$  on all lattices with size  $L$  not smaller than a given  $L_{\min}$  according to the scaling law

$$\chi_L^{(M)} = AL^{\gamma/\nu} \ln^r L. \quad (21)$$

---

<sup>2</sup>The symbol  $\beta$  here denotes a critical index and not, obviously, the coupling of the theory. In spite of this inconvenient notation, we are confident that no confusion will arise, since it will be always clear from the context which  $\beta$  is to be referred to.

As the value of the critical coupling  $\beta_c^{(1)}$  we use the central value of the determination from the method (b) (see Table 3).

The results of the fits are summarized in Tables 4, 5, 6, 7, for the cases of  $Z(5)$  with  $N_t=2$ ,  $Z(5)$  with  $N_t=4$ ,  $Z(7)$  with  $N_t=2$  and  $Z(7)$  with  $N_t=4$ , respectively. The reference value for the index  $\eta$  at this transition is  $1/4$ , whereas the hyperscaling relation to be fulfilled is  $\gamma/\nu + 2\beta/\nu = d = 2$ .

The procedure for the determination of the critical indices at the second transition is similar to the one for the first transition, with the difference that the fit with the scaling laws Eqs. (20) and (21) is to be applied to data of the rotated magnetization,  $M_R$ , and of its susceptibility,  $\chi_L^{(M_R)}$ , respectively. As the value of the critical coupling  $\beta_c^{(2)}$  we use the one determined from the method (e) (see Table 3).

The results of the fits are summarized in Tables 8, 9, 10, 11, for the cases of  $Z(5)$  with  $N_t=2$ ,  $Z(5)$  with  $N_t=4$ ,  $Z(7)$  with  $N_t=2$  and  $Z(7)$  with  $N_t=4$ , respectively. The reference value for the index  $\eta$  at this transition is  $4/N^2$ , *i.e.*  $\eta = 0.16$  for  $N = 5$  and  $\eta = 0.0816..$  for  $N = 7$ , whereas the hyperscaling relation to be fulfilled is  $\gamma/\nu + 2\beta/\nu = d = 2$ .

A general comment is that in many of the cases we investigated both  $d$  and  $\eta$  at the two critical points slightly differ from the expected values, though these differences cancel to a large extent if we define  $\eta$  as  $2\beta/\nu$ .

There is an independent method to determine the critical exponent  $\eta$ , which does not rely on the prior knowledge of the critical coupling, but is based on the construction of a suitable universal quantity [28, 21]. The idea is to plot  $\chi_L^{(M_R)} L^{\eta-2}$  versus  $B_4^{(M_R)}$  and to look for the value of  $\eta$  which optimizes the overlap of curves from different volumes. This method is illustrated in Fig. 8 for the case of  $Z(7)$  with  $N_t = 4$ : for  $\eta = 0.25$  the overlap is optimal in the lower branch of the curves, corresponding to the region of the first transition, while per  $\eta = 0.0816 \simeq 4/7^2$  the overlap is optimal in the upper branch. Another option is to plot  $M_R L^{\eta/2}$  versus  $m_\psi$ , which leads to overlapping curves for  $\eta$  fixed at the value of the second phase transition, as illustrated in Fig. 9 for the case of  $Z(7)$  with  $N_t = 2$  and  $N_t = 4$ .



Table 4: Critical indices  $\beta/\nu$  and  $\gamma/\nu$  for the first transition in  $Z(5)$  with  $N_t = 2$ , determined by the fits given in Eqs. (20) and (21) on the complex magnetization  $M_L$  and its susceptibility  $\chi_L^{(M)}$  at  $\beta_c^{(1)} = 1.87$  for different choices of the minimum lattice size  $L_{\min}$  (an asterisk indicates a fixed parameter). The  $\chi^2$  of the two fits, given in the columns four and seven, is the reduced one.

$L_{\min}$	$\beta/\nu$	$r_{\beta/\nu}$	$\chi_{\beta/\nu}^2$	$\gamma/\nu$	$r_{\gamma/\nu}$	$\chi_{\gamma/\nu}^2$	$d = 2\beta/\nu + \gamma/\nu$	$\eta = 2 - \gamma/\nu$
16	0.12040(7)	0*	4.43	1.692(2)	0*	52.74	1.933(2)	0.308(2)
	0.1228(5)	0.013(3)	2.43	1.97(1)	-1.44(6)	0.90	2.22(1)	0.03(1)
				1.668(2)	0.125*	61.75	1.908(2)	0.332(2)
32	0.12047(8)	0*	4.49	1.712(2)	0*	22.49	1.953(2)	0.288(2)
	0.1239(7)	0.019(4)	2.12	1.97(2)	-1.4(1)	0.99	2.22(2)	0.03(2)
				1.690(2)	0.125*	26.40	1.931(2)	0.310(2)
64	0.1206(1)	0*	4.30	1.729(3)	0*	6.93	1.970(3)	0.271(3)
	0.126(1)	0.034(7)	1.51	1.93(3)	-1.2(2)	0.73	2.18(3)	0.07(3)
				1.708(3)	0.125*	8.30	1.949(3)	0.292(3)
128	0.1208(1)	0*	2.43	1.740(3)	0*	3.00	1.982(3)	0.260(3)
	0.126(2)	0.03(1)	1.72	1.94(9)	-1.3(5)	0.84	2.19(9)	0.06(9)
				1.720(3)	0.125*	3.48	1.962(3)	0.280(3)
192	0.1210(1)	0*	2.09	1.745(4)	0*	1.97	1.987(4)	0.255(4)
	0.125(3)	0.03(2)	2.06	1.91(4)	-1.1(2)	0.97	2.16(4)	0.09(4)
				1.726(4)	0.125*	2.25	1.968(4)	0.274(4)
256	0.1211(2)	0*	2.19	1.752(5)	0*	1.44	1.994(5)	0.248(5)
	0.124(4)	0.02(3)	2.56	1.906(5)	-1.02(3)	1.19	2.15(1)	0.094(5)
				1.733(5)	0.125*	1.56	1.975(5)	0.267(5)
384	0.1212(2)	0*	2.44	1.758(6)	0*	1.02	2.000(6)	0.242(6)
	0.1224(2)	0.0079(9)	3.27	1.836(6)	-0.53(3)	1.37	2.080(6)	0.164(6)
				1.740(6)	0.125*	1.04	1.982(6)	0.260(6)
512	0.1215(3)	0*	2.18	1.762(7)	0*	1.06	2.005(8)	0.238(7)
	0.1021(2)	-0.135(1)	1.21	1.840(6)	-0.54(3)	1.88	2.044(7)	0.160(6)
				1.744(7)	0.125*	1.02	1.987(8)	0.256(7)
768	0.1209(4)	0*	1.71	1.76(1)	0*	1.49	2.00(1)	0.24(1)
	0.1220(3)	0.008(1)	3.52	1.834(8)	-0.54(3)	3.24	2.078(8)	0.166(8)
				1.74(1)	0.125*	1.47	1.98(1)	0.26(1)
1024	0.1209(6)	0*	3.41	1.76(2)	0*	2.93	2.00(2)	0.24(2)
				1.74(2)	0.125*	2.89	1.98(2)	0.26(2)

Table 5: The same as Table 4 for  $Z(5)$  with  $N_t = 4$ , determined at  $\beta_c^{(1)} = 2.813$ .

$L_{\min}$	$\beta/\nu$	$r_{\beta/\nu}$	$\chi_{\beta/\nu}^2$	$\gamma/\nu$	$r_{\gamma/\nu}$	$\chi_{\gamma/\nu}^2$	$d = 2\beta/\nu + \gamma/\nu$	$\eta = 2 - \gamma/\nu$
128	0.1215(2)	0*	0.45	1.730(5)	0*	1.23	1.973(5)	0.270(5)
	0.126(4)	0.02(2)	0.30	1.808(6)	-0.46(3)	1.36	2.06(1)	0.192(6)
				1.709(5)	0.125*	1.32	1.952(5)	0.291(5)
192	0.1217(3)	0*	0.25	1.734(6)	0*	1.20	1.977(7)	0.266(6)
	0.1228(3)	0.007(1)	0.32	1.707(7)	0.17(3)	1.59	1.952(7)	0.293(7)
				0.25	1.714(6)	0.125*	1.19	1.957(7)
256	0.1218(3)	0*	0.30	1.740(8)	0*	1.07	1.983(8)	0.260(8)
	0.1229(3)	0.007(1)	0.47	1.62(3)	0.7(2)	0.88	1.87(3)	0.38(3)
				1.720(8)	0.125*	0.98	1.963(8)	0.280(8)
384	0.1217(5)	0*	0.44	1.73(1)	0*	0.24	1.97(1)	0.27(1)
	0.1228(4)	0.007(2)	0.86	1.785(9)	-0.38(4)	0.62	2.03(1)	0.215(9)
				1.71(1)	0.125*	0.22	1.95(1)	0.29(1)
512	0.1220(7)	0*	0.49	1.72(2)	0*	0.05	1.96(2)	0.28(2)
				1.70(2)	0.125*	0.05	1.94(2)	0.30(2)

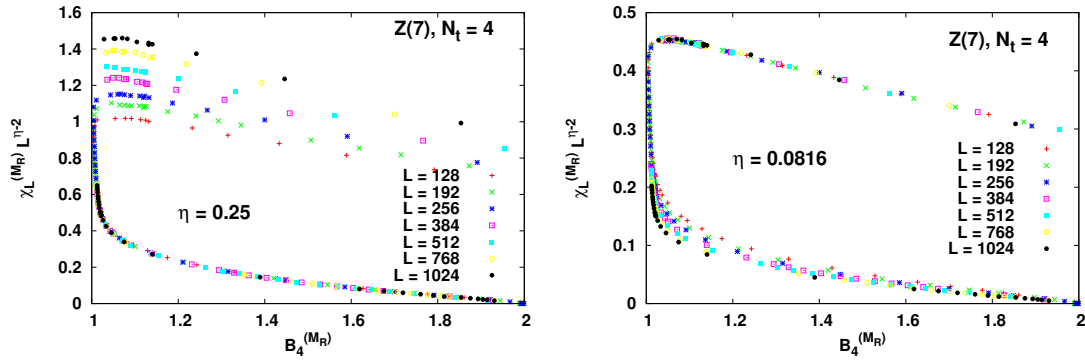


Figure 8: Correlation between  $\chi_L^{(M_R)} L^{\eta-2}$  and the Binder cumulant  $B_4^{(M_R)}$  in  $Z(7)$  with  $N_t = 4$  for  $\eta = 0.25$  (left) and for  $\eta = 0.0816$  (right) on lattices with  $L$  ranging from 128 to 1024.

Table 6: The same as Table 4 for  $Z(7)$  with  $N_t = 2$ , determined at  $\beta_c^{(1)} = 2.031$ .

$L_{\min}$	$\beta/\nu$	$r_{\beta/\nu}$	$\chi_{\beta/\nu}^2$	$\gamma/\nu$	$r_{\gamma/\nu}$	$\chi_{\gamma/\nu}^2$	$d = 2\beta/\nu + \gamma/\nu$	$\eta = 2 - \gamma/\nu$
128	0.12862(9)	0*	11.95	1.768(2)	0*	0.93	2.025(2)	0.232(2)
	0.141(1)	0.078(9)	0.93	1.763(2)	0.030(3)	1.15	2.045(5)	0.237(2)
				1.747(2)	0.125*	1.18	2.004(2)	0.253(2)
192	0.1290(1)	0*	7.73	1.767(3)	0*	1.09	2.025(3)	0.233(3)
	0.143(2)	0.09(1)	0.87	1.89(2)	-0.8(1)	0.33	2.17(3)	0.11(2)
				1.748(3)	0.125*	1.36	2.006(3)	0.252(3)
256	0.1294(1)	0*	5.84	1.771(4)	0*	0.83	2.029(4)	0.229(4)
	0.145(3)	0.10(2)	0.95	1.87(3)	-0.6(2)	0.44	2.16(3)	0.13(3)
				1.752(4)	0.125*	1.00	2.010(4)	0.248(4)
384	0.1297(2)	0*	4.96	1.775(5)	0*	0.58	2.034(5)	0.225(5)
	0.1517(2)	0.1480(8)	0.27	1.865(5)	-0.61(2)	0.55	2.168(5)	0.135(5)
				1.757(5)	0.125*	0.64	2.016(5)	0.243(5)
512	0.1303(2)	0*	2.43	1.775(6)	0*	0.77	2.035(7)	0.225(6)
	0.1504(2)	0.1389(9)	0.38	1.94(6)	-1.2(4)	0.32	2.25(6)	0.06(6)
				1.757(6)	0.125*	0.86	2.017(7)	0.243(6)
768	0.1309(4)	0*	0.76	1.784(9)	0*	0.01	2.05(1)	0.216(9)
	0.1308(2)	-0.001(1)	1.54	1.875(6)	-0.65(3)	0.00	2.137(7)	0.125(6)
				1.767(9)	0.125*	0.01	2.03(1)	0.233(9)
1024	0.1311(5)	0*	1.36	1.79(1)	0*	0.00	2.05(2)	0.21(1)
				1.77(1)	0.125*	0.01	2.03(2)	0.23(1)

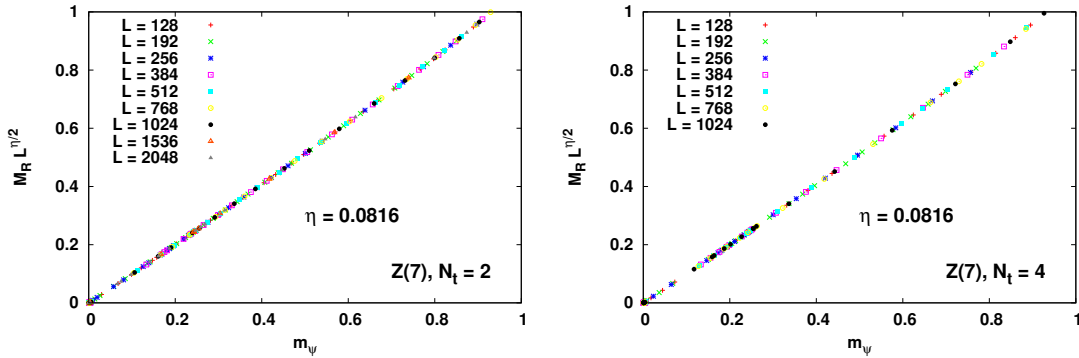


Figure 9: Correlation between  $M_R L^{\eta/2}$  and  $m_\psi$  in  $Z(7)$  with  $N_t = 2$  (left) and in  $Z(7)$  with  $N_t = 4$  (right) for  $\eta = 0.0816$  on lattices with various values of  $L$ .

Table 7: The same as Table 4 for  $Z(7)$  with  $N_t = 4$ , determined at  $\beta_c^{(1)} = 3.406$ .

$L_{\min}$	$\beta/\nu$	$r_{\beta/\nu}$	$\chi_{\beta/\nu}^2$	$\gamma/\nu$	$r_{\gamma/\nu}$	$\chi_{\gamma/\nu}^2$	$d = 2\beta/\nu + \gamma/\nu$	$\eta = 2 - \gamma/\nu$
128	0.1294(1)	0*	4.64	1.772(3)	0*	1.72	2.031(4)	0.228(3)
	0.141(2)	0.07(1)	0.54	1.766(4)	0.04(2)	2.16	2.049(9)	0.234(4)
				1.751(3)	0.125*	1.76	2.010(4)	0.249(3)
192	0.1298(2)	0*	3.61	1.771(5)	0*	2.12	2.031(5)	0.229(5)
	0.1456(2)	0.0961(8)	0.20	1.85(8)	-0.5(5)	2.64	2.14(8)	0.15(8)
				1.751(5)	0.125*	2.20	2.010(5)	0.249(5)
256	0.1302(2)	0*	1.43	1.778(6)	0*	1.84	2.038(6)	0.222(6)
	0.1432(2)	0.0811(9)	0.19	1.74(3)	0.2(2)	2.58	2.03(3)	0.26(3)
				1.758(6)	0.125*	1.77	2.018(6)	0.242(6)
384	0.1307(3)	0*	0.37	1.773(9)	0*	2.48	2.03(1)	0.227(9)
	0.1303(2)	-0.003(1)	0.78	1.871(7)	-0.63(3)	5.32	2.132(7)	0.129(7)
				1.754(9)	0.125*	2.45	2.01(1)	0.246(9)
512	0.1310(5)	0*	0.08	1.78(1)	0*	4.86	2.04(1)	0.22(1)
				1.76(1)	0.125*	4.77	2.02(1)	0.24(1)

Table 8: Critical indices  $\beta/\nu$  and  $\gamma/\nu$  for the second transition in  $Z(5)$  with  $N_t = 2$ , determined by the fits given in Eqs. (20) and (21) on the rotated magnetization  $M_R$  and its susceptibility  $\chi_L^{(M_R)}$  at  $\beta_c^{(2)} = 1.940$  for different choices of the minimum lattice size  $L_{\min}$  (an asterisk indicates a fixed parameter).

$L_{\min}$	$\beta/\nu$	$r_{\beta/\nu}$	$\chi_{\beta/\nu}^2$	$\gamma/\nu$	$r_{\gamma/\nu}$	$\chi_{\gamma/\nu}^2$	$d = 2\beta/\nu + \gamma/\nu$	$\eta = 2 - \gamma/\nu$
128	0.037(8)	0*	2.22	1.918(2)	0*	0.52	1.99(2)	0.082(2)
	-0.27(3)	-1.8(2)	1.07	1.900(3)	0.11(1)	0.53	1.36(7)	0.100(3)
192	0.03(1)	0*	2.10	1.918(3)	0*	0.64	1.97(2)	0.082(3)
	-0.25(4)	-1.6(2)	1.52	1.821(3)	0.59(1)	0.31	1.33(8)	0.179(3)
256	0.01(1)	0*	2.27	1.916(4)	0*	0.64	1.94(3)	0.084(4)
	-0.20(5)	-1.3(3)	2.38	1.900(3)	0.10(1)	0.82	1.5(1)	0.100(3)
384	-0.02(2)	0*	1.77	1.913(6)	0*	0.62	1.88(5)	0.087(6)
	-0.01(2)	0.03(6)	3.56	1.87(3)	0.3(2)	1.06	1.85(6)	0.13(3)
512	-0.05(3)	0*	1.37	1.912(8)	0*	1.21	1.81(7)	0.088(8)

Table 9: The same as Table 8 for  $Z(5)$  with  $N_t = 4$ , determined at  $\beta_c^{(2)} = 2.898$ .

$L_{\min}$	$\beta/\nu$	$r_{\beta/\nu}$	$\chi_{\beta/\nu}^2$	$\gamma/\nu$	$r_{\gamma/\nu}$	$\chi_{\gamma/\nu}^2$	$d = 2\beta/\nu + \gamma/\nu$	$\eta = 2 - \gamma/\nu$
128	0.17(1)	0*	1.52	1.850(3)	0*	0.07	2.20(3)	0.150(3)
	-0.28(5)	-2.6(3)	0.30	1.847(4)	0.02(2)	0.08	1.3(1)	0.153(4)
192	0.15(1)	0*	0.40	1.849(4)	0*	0.07	2.15(3)	0.151(4)
	-0.1(1)	-1.5(6)	0.25	1.847(4)	0.01(2)	0.09	1.6(2)	0.153(4)
256	0.15(2)	0*	0.51	1.849(5)	0*	0.07	2.14(4)	0.151(5)
	-0.09(9)	-1.5(5)	0.36	1.846(5)	0.01(2)	0.10	1.7(2)	0.154(5)
384	0.12(3)	0*	0.24	1.847(8)	0*	0.07	2.09(7)	0.153(8)
	0.10(2)	-0.15(9)	0.45	1.845(6)	0.01(2)	0.14	2.04(5)	0.155(6)
512	0.10(5)	0*	0.21	1.85(1)	0*	0.11	2.1(1)	0.15(1)

Table 10: The same as Table 8 for  $Z(7)$  with  $N_t = 2$ , determined at  $\beta_c^{(2)} = 3.366$ .

$L_{\min}$	$\beta/\nu$	$r_{\beta/\nu}$	$\chi_{\beta/\nu}^2$	$\gamma/\nu$	$r_{\gamma/\nu}$	$\chi_{\gamma/\nu}^2$	$d = 2\beta/\nu + \gamma/\nu$	$\eta = 2 - \gamma/\nu$
128	0.034(6)	0*	2.33	1.921(2)	0*	0.45	1.99(1)	0.079(2)
	-0.27(5)	-1.9(3)	0.34	1.89(3)	0.2(2)	0.27	1.3(1)	0.11(3)
192	0.018(7)	0*	0.72	1.919(2)	0*	0.23	1.96(2)	0.081(2)
	-0.19(4)	-1.3(3)	0.26	1.903(2)	0.10(1)	0.26	1.53(9)	0.097(2)
256	0.010(9)	0*	0.26	1.919(2)	0*	0.28	1.94(2)	0.081(2)
	-0.12(7)	-0.8(4)	0.18	1.904(3)	0.10(1)	0.28	1.7(1)	0.096(3)
384	0(1)	0*	11.54	1.919(3)	0*	0.35	2(2)	0.081(3)
	-0.12(6)	-0.9(4)	0.21	1.904(3)	0.10(1)	0.37	1.7(1)	0.096(3)
512	0.00(2)	0*	0.25	1.917(4)	0*	0.21	1.92(3)	0.083(4)
	0.00(1)	0.00(5)	0.38	1.903(3)	0.10(1)	0.29	1.91(3)	0.097(3)
768	-0.01(2)	0*	0.11	1.916(6)	0*	0.29	1.90(5)	0.084(6)
	-0.01(1)	0.02(6)	0.22	1.903(4)	0.10(2)	0.56	1.89(3)	0.097(4)
1024	-0.00(3)	0*	0.14	1.918(8)	0*	0.53	1.91(7)	0.082(8)

Table 11: The same as Table 8 for  $Z(7)$  with  $N_t = 4$ , determined at  $\beta_c^{(2)} = 5.158$ .

$L_{\min}$	$\beta/\nu$	$r_{\beta/\nu}$	$\chi_{\beta/\nu}^2$	$\gamma/\nu$	$r_{\gamma/\nu}$	$\chi_{\gamma/\nu}^2$	$d = 2\beta/\nu + \gamma/\nu$	$\eta = 2 - \gamma/\nu$
128	0.037(8)	0*	2.22	1.918(2)	0*	0.52	1.99(2)	0.082(2)
	-0.27(3)	-1.8(2)	1.07	1.900(3)	0.11(1)	0.53	1.36(7)	0.100(3)
192	0.03(1)	0*	2.10	1.918(3)	0*	0.64	1.97(2)	0.082(3)
	-0.25(4)	-1.6(2)	1.52	1.821(3)	0.59(1)	0.31	1.33(8)	0.179(3)
256	0.01(1)	0*	2.27	1.916(4)	0*	0.64	1.94(3)	0.084(4)
	-0.20(5)	-1.3(3)	2.38	1.900(3)	0.10(1)	0.82	1.5(1)	0.100(3)
384	-0.02(2)	0*	1.77	1.913(6)	0*	0.62	1.88(5)	0.087(6)
	-0.01(2)	0.03(6)	3.56	1.87(3)	0.3(2)	1.06	1.85(6)	0.13(3)
512	-0.05(3)	0*	1.37	1.912(8)	0*	1.21	1.81(7)	0.088(8)

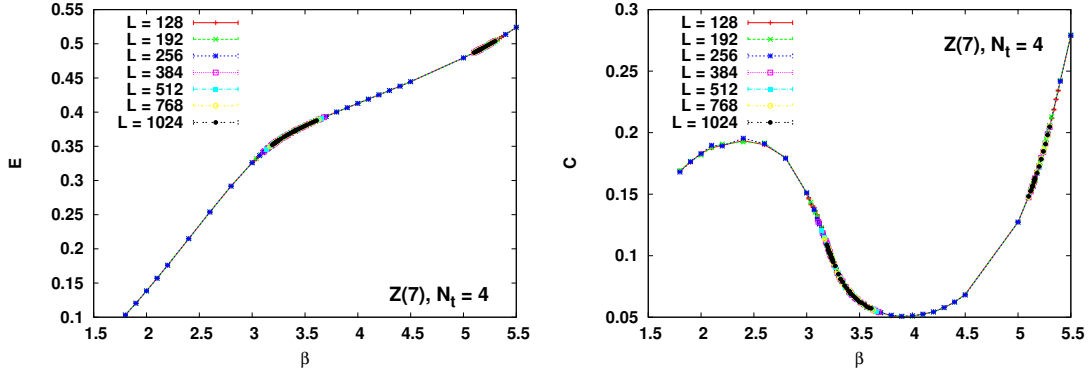


Figure 10: Mean link energy (left) and specific heat (right) versus  $\beta$  in  $Z(7)$  with  $N_t = 4$  on lattices with  $L$  ranging from 128 to 1024.

Table 12: Summary of the known values of the critical couplings  $\beta_c^{(1)}$  and  $\beta_c^{(2)}$  in  $Z(N)$  with  $N_t = 2, 4$ .

$N$	$N_t$	$\beta_c^{(1)}$	$\beta_c^{(2)}$	Reference
5	2	1.87(1)	1.940(7)	this work
7	2	2.031(7)	3.366(7)	this work
9	2	2.04(3)	5.38(4)	this work
13	2	2.02(1)	10.815(8)	this work
$\infty$	2	–	$\infty$	
5	4	2.813(3)	2.898(4)	this work
7	4	3.406(8)	5.158(7)	this work
9	4	3.50(1)	8.28(1)	this work
13	4	3.490(6)	16.94(2)	this work
$\infty$	4	3.42(1)	$\infty$	[9]

### 3.4 Other checks of the nature of the phase transitions

To produce further evidence in favor of the fact that the phase transitions investigated so far are both of infinite order, we have calculated the mean link energy  $E$  and the specific heat  $C$  around the transitions in  $Z(5)$  and in  $Z(7)$  with  $N_t=2$  and  $N_t = 4$  (see Fig. 10 for the case of  $Z(7)$  with  $N_t = 4$ , for example). In all cases the dependence of  $E$  and  $C$  on  $\beta$  is continuous, so that first and second order transitions are ruled out.

## 4 Behavior with $N$ of the critical couplings

The results of this work and those available in the literature allow us to make some considerations about the behavior with  $N$  of the critical couplings  $\beta_c^{(1)}$  and  $\beta_c^{(2)}$ . Examining our data for  $\beta_c^{(1,2)}$ , one concludes that, for a fixed  $N_t$ ,

- $\beta_c^{(1)}$  converges to the  $XY$  value very fast, like  $\exp(-aN^2)$  ,
- $\beta_c^{(2)}$  diverges like  $N^2$  .

To better see the dependence on  $N$  of the critical couplings, we have found also the critical coupling  $\beta_c^{(1,2)}$  in  $Z(9)$  and  $Z(13)$  with  $N_t = 2$  and  $N_t = 4$ , using the method (b) for  $\beta_c^{(1)}$  and the method (e) for  $\beta_c^{(2)}$  (see Section 3.3 for the details of these methods). In Table 12 we summarize the present knowledge about the position of the critical points for  $3d$   $Z(N)$  gauge models at  $\beta_s = 0$ .

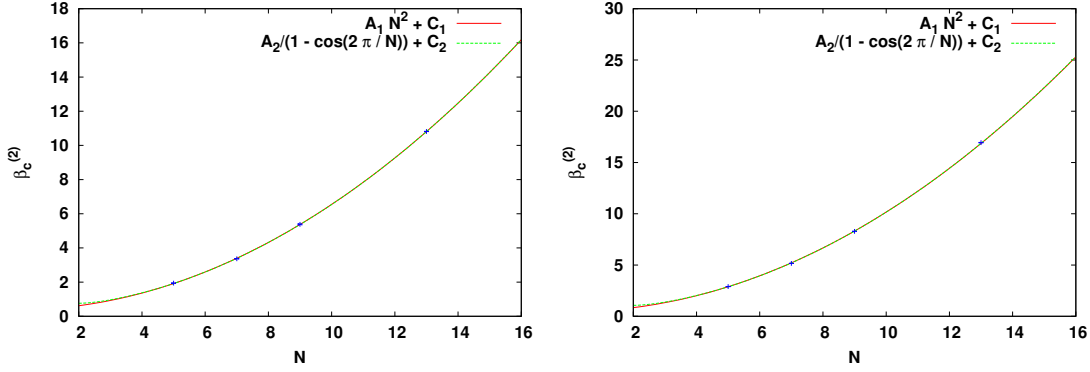


Figure 11: Fits of critical values for  $\beta_c^{(2)}$  as a function of  $N$  for  $N_t = 2$  (left) and  $N_t = 4$  (right).

One should expect that the  $3d$   $Z(N)$  gauge models at  $\beta_s = 0$  satisfy the scaling predicted by RG, probably up to  $\mathcal{O}(N)$  corrections. One could try therefore to fit the available Monte Carlo data for  $\beta_c^{(1,2)}$  with formulae predicted by RG and modified to account for such corrections.

We find that the critical couplings for the first transition are well reproduced by the function

$$\beta_c^{(1)} = A - BN^2 \exp\left(-\frac{N^2}{C}\right),$$

for suitable values of the parameters  $A$ ,  $B$  and  $C$ , both for  $N_t = 2$  and  $N_t = 4$ .

The critical couplings for the second transition are well reproduced instead by the following functions:

$$\beta_c^{(2)} = AN^2 + BN + C$$

and

$$\beta_c^{(2)} = \frac{A}{1 - \cos\left(\frac{2\pi}{N}\right)} + BN + C,$$

for suitable values of the parameters  $A$ ,  $B$  and  $C$ , both for  $N_t = 2$  and  $N_t = 4$ . The last formula has been suggested in Ref. [1] in the context of the zero-temperature theory.

As an illustration of our fits, Fig. 11 shows the dependence of  $\beta_c^{(2)}$  on  $N$  (parameter  $B = 0$  in fitting formulas). One concludes from these plots that to distinguish between two scalings one should probably have data for smaller values of  $N = 2, 3, 4$  at  $\beta_s = 0$ .



## 5 Conclusions

In this paper we have studied the  $3d$   $Z(N)$  gauge theory at the finite temperature in the strong coupling region  $\beta_s = 0$ . This study was based on the exact relation of this model to a generalized  $2d$   $Z(N)$  spin model. In Section 2 we established the exact relation between couplings of these two models, described qualitatively some of the RG predictions for effective model and gave analytical estimations of the critical couplings.

The main, numerical part of the work has been devoted to the localization of the critical couplings and to the computation of the critical indices:

- We have determined numerically the two critical couplings of  $Z(N = 5, 7, 9, 13)$  LGTs and given estimates of the critical indices  $\eta$  at both transitions. For the first time we have a clear indication that for all  $N \geq 5$  the scenario of three phases is realized: a disordered phase at small  $\beta_t$ , a massless or BKT one at intermediate values of  $\beta_t$  and an ordered phase, occurring at larger and larger values of  $\beta_t$  as  $N$  increases. This matches perfectly with the  $N \rightarrow \infty$  limit, *i.e.* the finite-temperature  $3d$   $U(1)$  LGT (at  $\beta_s = 0$ ), where the ordered phase is absent;
- We have found that the values of the critical index  $\eta$  at the two transitions are compatible with the theoretical expectations; in order to reproduce the expected value of  $\eta$ , we had to take into account logarithmic corrections with the exponent  $r$  fixed to 0.125;
- The index  $\nu$  also appears to be compatible with the value  $1/2$ , in agreement with RG predictions.

Results listed above present further evidence that finite-temperature  $3d$   $Z(N)$  LGTs for  $N > 4$  undergo two phase transitions of the BKT type.

Moreover, this model belongs to the universality class of the  $2d$   $Z(N)$  spin model, at least in the strong coupling limit  $\beta_s = 0$ .

Considering the determinations of the critical couplings as a function of  $N$ , we have conjectured the approximate scaling for  $\beta_c^{(1,2)}(N)$ .

Finally, the study performed here allows to improve our knowledge of the phase diagrams of the generalized  $2d$   $Z(N)$  spin models. As an example, we plot in Fig. 12 the general phase diagram for  $N = 5$  in the  $(t_1, t_2)$ -plane, where  $t_i = (B_i/B_0)^{N_t}$ , and  $B_i$  are defined in (7). Here, the line  $AB$  is self-dual line, SPM corresponds to the standard Potts model, VPM to the vector model. The SPM undergoes a first order phase transition with a critical point occurring on the self-dual line. The line of the first order phase transition terminates at the point 2. Its approximate position was computed in Ref. [29]. Shown are also the locations of the critical points for the VPM ( $N_t = 1$ ) and for  $Z(5)$  LGT with  $N_t = 2, 4$ . The parametric curves for different  $N_t$  lie very close to each other, so we cannot

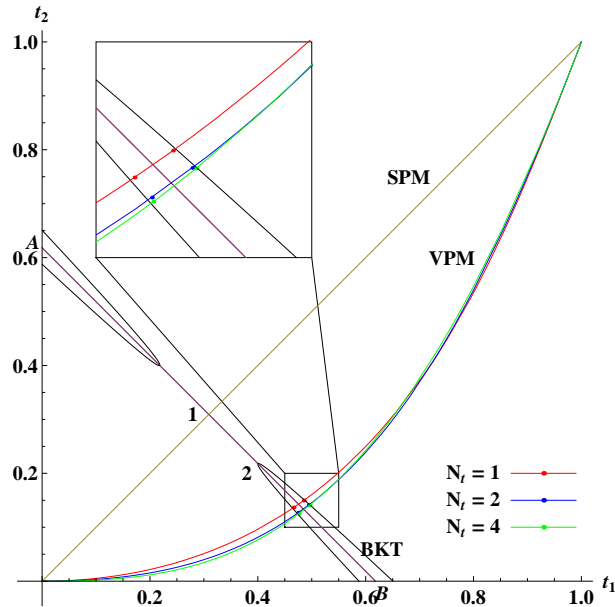


Figure 12: Phase structure of the general  $Z(5)$  spin model (see text for explanation).

trace a sufficiently big part of the curve while changing  $N_t$ . On the other hand it shows that already the model with  $N_t = 4$  presents a very good approximation to the finite-temperature limit. Indeed, the parametric curve for  $N_t = 8$  is almost indistinguishable from the curve with  $N_t = 4$ .

## 6 Acknowledgments

The work of O.B. was supported by the Program of Fundamental Research of the Department of Physics and Astronomy of NAS, Ukraine. The work of G.C. and M.G. was supported in part by the European Union under ITN STRONGnet (grant PITN-GA-2009-238353). G.C. thanks Matteo Giordano for useful discussions.

## References

- [1] G. Bhanot and M. Creutz, Phys. Rev. D **21** (1980) 2892.
- [2] A. Polyakov, Nucl. Phys. B **120** (1977) 429; T. Banks, J. Kogut, R. Myerson, Nucl. Phys. B **121** (1977) 493; M. Göpfert, G. Mack, Commun. Math. Phys. **81** (1981) 97.
- [3] B. Svetitsky, L. Yaffe, Nucl. Phys. B **210** (1982) 423.

- [4] V. Berezinskii, Sov. Phys. JETP **32** (1971) 493.
- [5] J. Kosterlitz, D. Thouless, J. Phys. C **6** (1973) 1181.
- [6] J. Kosterlitz, J. Phys. C **7** (1974) 1046.
- [7] N. Parga, Phys. Lett. B **107** (1981) 442.
- [8] O. Borisenko, *Critical behaviour of 3D U(1) LGT at finite temperature*, PoS LAT **2007** (2007) 170.
- [9] O. Borisenko, M. Gravina, A. Papa, J. Stat. Mech. **2008** (2008) P08009.
- [10] O. Borisenko, R. Fiore, M. Gravina, A. Papa, J. Stat. Mech. **2010** (2010) P04015.
- [11] F.Y. Wu, Rev. Mod. Phys. **54** (1982) 235.
- [12] S. Elitzur, R.B. Pearson, J. Shigemitsu, Phys. Rev. D **19** (1979) 3698.
- [13] M. B. Einhorn, R. Savit, and E. Rabinovici, Nucl. Phys. B **170** (1980) 16.
- [14] C.J. Hamer, J.B. Kogut, Phys. Rev. B **22** (1980) 3378.
- [15] B. Nienhuis, J. Statist. Phys. **34** (1984) 731.
- [16] L.P. Kadanoff, J. Phys. A **11** (1978) 1399.
- [17] J.L. Cardy, J. Phys. A **13** (1980) 1507.
- [18] J. Fröhlich, T. Spencer, Commun. Math. Phys. **81** (1981) 527.
- [19] Y. Tomita, Y. Okabe, Phys. Rev. B **65** (2002) 184405.
- [20] O. Borisenko, G. Cortese, R. Fiore, M. Gravina, A. Papa, *Critical properties of the two-dimensional Z(5) vector model*, PoS LATTICE **2010** (2010) 274 [arXiv:1101.0512 [hep-lat]].
- [21] O. Borisenko, G. Cortese, R. Fiore, M. Gravina and A. Papa, Phys. Rev. E **83** (2011) 041120.
- [22] O. Borisenko, G. Cortese, R. Fiore, M. Gravina, A. Papa, *Critical properties of 2D Z(N) models for N > 4*, PoS LATTICE **2011** (2011) 304 [arXiv:1110.6385 [hep-lat]].
- [23] O. Borisenko, V. Chelnokov, G. Cortese, R. Fiore, M. Gravina, A. Papa, Phys. Rev. E **85** (2012) 021114.

- [24] M. Billò, M. Caselle, A. D'Adda, *Int. J. Mod. Phys. A* **12** (1997) 5753.
- [25] A. Yamagata and I. Ono, *J. Phys.* **A24** (1991) 265.
- [26] R. Kenna and A. C. Irving, *Nucl. Phys. B* **485** (1997) 583.
- [27] M. Hasenbusch, *J. Phys. A* **38** (2005) 5869.
- [28] D. Loison, *J. Phys.: Condens. Matter* **11** (1999) L401.
- [29] E. Domany, D. Mukamel, A. Schwimmer, *J. Phys. A* **13** (1980) L311.